Continuation Power Flow Analysis of Power System Voltage Stability with Unified Power Flow Controller

Youcef Islam Djilani Kobibi[1*] , Mohamed Abdeldjalil Djehaf[2] , Mohamed Khatir[2] , Mohamed Ouadafraksou[3]

[1] Department of Electrical Engineering, Faculty of Sciences and Technology, Mustapha Stambouli University, 29000 Mascara, Algeria

[2] Department of Automatic Control, Faculty of Electrical Engineering, Djillali Liabes University, 22000 Sidi Bel-Abbes, Algeria

[3] Department of Electrical Engineering, Faculty of Electrical-Electronics, Sakarya University, 54050 Sakarya, Turkey

* Correspondence: Youcef Islam Djilani Kobibi (y.djilani.kobibi@univ-mascara.dz)

Abstract: The rising power demand has forced power systems all over the world to operate very close to their stability limits. When power systems are overloaded, faulty, or in lack of reactive power, voltage collapses would ensue. The capacity of a power system to keep the voltage of every bus constant under disturbances is called voltage stability. This dynamic phenomenon hinges on the load features. It is commonly known that flexible AC transmission systems (FACTS) can improve voltage stability. This paper puts forward a load flow model with the unified power flow controller (UPFC), and relies on the model to investigate the voltage stability of a power system through continuation power flow (CPF) method. The validity of the model was verified through a simulation, using the power system analysis toolbox (PSAT) in MATLAB/Simulink environment.

Keywords: Flexible AC transmission systems (FACTS); Unified power flow controller (UPFC); Continuation power flow (CPF); Voltage stability; P-V curve

1. Introduction

Facing the rising demand for electrical energy, it is increasingly challenging for the power transmission systems to respond with high stability and good controllability. The current transmission infrastructure is already strained, trying to meet the growing power demand. Power system engineers are primarily concerned with the quality and quantity of the power supply. To ensure the quality of the delivered power, the system features a few control mechanisms that bring the temperature and stability constraints closer [1, 2].

The bus voltage may drop to a point where it cannot recover when a system is overloaded and already under stress. This can result in voltage collapse and, if ignored, system termination [3]. This viewpoint contends that improved levels of quality, dependability, and stability provided by new developments in power electronic equipment can be advantageous to the power system [4].

Over the past ten years, the power electronic has developed into an all-purpose solution to all problems and limitations. Flexible AC transmission systems (FACTS) based on power electronics are mainly converters or thyristor-controlled devices that manage the X-mission and distribution power flow as well as other system variable features like X-mission reactance, phase angle, and voltage [5]. The unified power flow controller (UPFC) is widely regarded as the most effective FACTS, thanks to its ability to control all three factors simultaneously [6].

With the development of UPFC concepts, it is important to devise new methods for power flow analysis on the power system with UPFCs. Several researchers have tried to improve voltage stability using FACTS devices. Pereira et al. [7] assessed the dynamic voltage stability for a power system, including shunt FACTS devices like static compensator (STATCOM) and static var compensation (SVC). Fei et al. [8] presented a coordinated control

strategy for multi-objective voltage stability of series FACTS devices. Aydin and Gumus [9] developed a location-based algorithm to enhance the voltage stability of a power system using a shunt device.

This paper incorporates a series-shunt (hybrid) device in continuation power flow (CPF) analysis, and investigates the impact of the UPFC on voltage stability. After illustrating a CPF procedure, the authors put forward a UPFC load flow model. To measure the effect of loadability on system stability limit, a simulation was carried out using the power system analysis toolbox (PSAT) in MATLAB environment for a power system with and without the UPFC.

2. Unified Power Flow Controller

2.1 Operating Principal

The UPFC, which consists of a static compensator and a static series compensation, concurrently functions as a phase-shifting device and a shunt-compensating device.
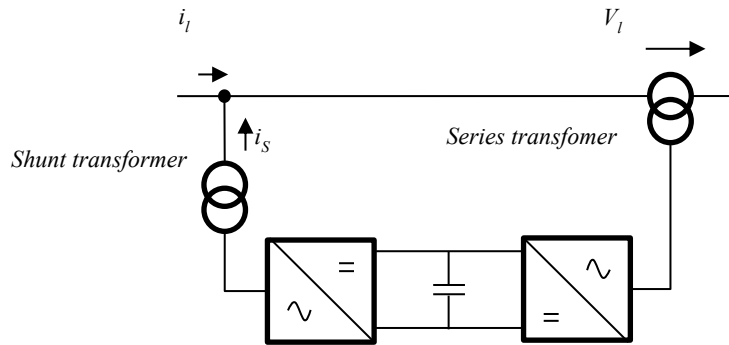

Figure 1. Sketch map of an UPFC

As shown in Figure 1, the UPFC is composed of a pair of converters, a shunt converter and a series converter. The two converters are connected by two voltage source converters and a common DC capacitor. Owing to the DC circuit, the active power exchange between the two converters controls the phase shift of the series voltage. This configuration assures the complete control over voltage and power flow. A thyristor bridge is required to protect the series converter. The number of real-world applications where both voltage and power flow control are required is constrained by the high cost of voltage source converters and protection, which makes a UPFC fairly expensive [10].

2.2 Load Flow Model

As shown in Figure 2 [11], the UPFC can be visualized as two ideal voltage sources: one voltage source V_{se} is connected in series to the transmission line, and the other voltage source V_{shu} injects the shunt current. Impedances in series with the voltage sources are used to mimic the coupling converter losses. Mathematically, the ideal voltage sources can be expressed as:

$$V_{shu} = V_{shu}(\cos\delta_{shu} + j\sin\delta_{shu})) \tag{1}$$

$$V_{se} = V_{se}(\cos\delta_{se} + j\sin\delta_{se})) \tag{2}$$

where, V_{shu} and δ_{shu} are the controllable magnitude and angle of the ideal voltage source of the shunt converter, respectively, which represent the shunt converter between the limits $0 \leq \delta_{shu} \leq 2\pi$ and $V_{shumin} \leq V_{shu} \leq V_{shumax}$; V_{se} and δ_{se} are the controllable magnitude and angle of the ideal voltage source of the series converter, respectively, representing the series converter between the limits $V_{semin} \leq V_{se} \leq V_{semax}$ and $0 \leq \delta_{se} \leq 2\pi$.

In the equivalent circuit of UPFC (Figure 2), the active and reactive powers at bus k can be respectively expressed as:

$$P_k = V_k^2 G_{kk} + V_k V_m (G_{km}\cos(\delta_k - \delta_m) + B_{km}\sin(\delta_k - \delta_m)) + V_k V_{shu}(G_{km}\cos(\delta_k - \delta_{shu})$$
$$+ B_{km}\sin(\delta_k - \delta_{shu})) + V_k V_{se}(G_{se}\cos(\delta_k - \delta_{se}) + B_{se}\sin(\delta_k - \delta_{se})) \tag{3}$$

$$Q_k = V_k^2 B_{kk} + V_k V_m (G_{km} \sin(\delta_k - \delta_m) - B_{km} \cos(\delta_k - \delta_m)) + V_k V_{shu} (G_{km} \sin(\delta_k - \delta_{shu})$$
$$-B_{km} \cos(\delta_k - \delta_{shu})) + V_k V_{se} (G_{se} \sin(\delta_k - \delta_{se}) - B_{se} \cos(\delta_k - \delta_{se})) \tag{4}$$

The active and reactive at bus *m* can be respectively expressed as:

$$P_m = V_m^2 G_{mm} + V_m V_k (G_{mk} \cos(\delta_m - \delta_k) + B_{mk} \sin(\delta_m - \delta_k)) + V_m V_{shu} (G_{mk} \cos(\delta_m - \delta_{shu})$$
$$+B_{mk} \sin(\delta_m - \delta_{shu})) + V_j V_{se} (G_{se} \cos(\delta_m - \delta_{se}) + B_{se} \sin(\delta_m - \delta_{se})) \tag{5}$$

$$Q_m = V_m^2 B_{mm} + V_m V_k (G_{mk} \sin(\delta_m - \delta_k) - B_{mk} \cos(\delta_m - \delta_k)) + V_m V_{sh} (G_{mk} \sin(\delta_m - \delta_{shu})$$
$$-B_{mk} \cos(\delta_m - \delta_{shu})) + V_m V_{se} (G_{se} \sin(\delta_m - \delta_{se}) - B_{se} \cos(\delta_m - \delta_{se})) \tag{6}$$

For the series converter, we have:

$$P_{se} = V_{se}^2 G_{mm} + V_{se} V_m (G_{mk} \cos(\delta_{se} - \delta_m) + B_{mk} \sin(\delta_{se} - \delta_m)) + V_{se} V_k (G_{kk} \cos(\delta_{se} - \delta_k)$$
$$+B_{kk} \sin(\delta_{se} - \delta_k)) \tag{7}$$

$$Q_{se} = -V_{se}^2 B_{kk} + V_{se} V_m (G_{mk} \sin(\delta_{se} - \delta_m) - B_{mk} \cos(\delta_{se} - \delta_m)) + V_{se} V_k (G_{kk} \sin(\delta_{se} - \delta_k)$$
$$-B_{kk} \cos(\delta_{se} - \delta_k)) \tag{8}$$

For the shunt converter, we have:

$$P_{shu} = -V_{shu}^2 G_{shu} + V_{shu} V_m (G_{sh} \cos(\delta_{shu} - \delta_m) + B_{sh} \sin(\delta_{shu} - \delta_m)) \tag{9}$$

$$Q_{shu} = V_{shu}^2 B_{shu} + V_{shu} V_m (G_{shu} \sin(\delta_{shu} - \delta_m) - B_{shu} \cos(\delta_{shu} - \delta_m)) \tag{10}$$

where, *G* and *B* are the corresponding conductance and susceptance, respectively.

Considering the losses of the converter valve, the active power P_{shu} supplied to the shunt converter is equivalent to 1.02 of the active power P_{se} required by the series converter:
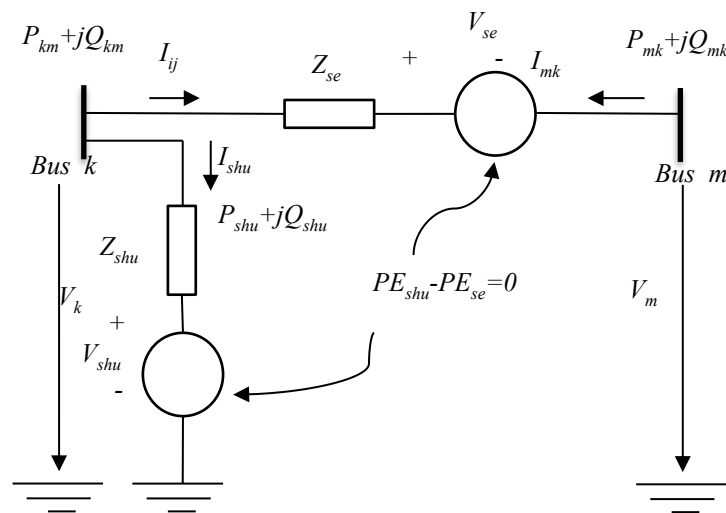
$$P_{shu} = -1.02 P_{se} \tag{11}$$

Figure 2. Equivalent circuit of UPFC

The linearized UPFC power equations are coupled with the equations of the AC network. Suppose bus m is a PQ bus. The UPFC involves the following variables: (1) voltage magnitude at the terminal of the shunt converter (bus k); (2) active power flow from bus m to bus k; (3) reactive power injected at bus m. Then, the linearized system of equations can be expressed as [12, 13]:

$$[J] = \begin{bmatrix} \dfrac{\partial P_i}{\partial \delta_i} & \dfrac{\partial P_i}{\partial \delta_j} & \dfrac{\partial P_i}{\partial V_{shu}}V_{shu} & \dfrac{\partial P_i}{\partial V_j}V_j & \dfrac{\partial P_i}{\partial \delta_{se}} & \dfrac{\partial P_i}{\partial V_{se}}V_{se} & \dfrac{\partial P_i}{\partial \delta_{shu}} \\[2ex] \dfrac{\partial P_k}{\partial \delta_m} & \dfrac{\partial P_m}{\partial \delta_m} & 0 & \dfrac{\partial P_m}{\partial V_m}V_m & \dfrac{\partial P_m}{\partial \delta_{se}} & \dfrac{\partial P_m}{\partial V_{se}}V_{se} & 0 \\[2ex] \dfrac{\partial Q_k}{\partial \delta_k} & \dfrac{\partial Q_k}{\partial \delta_m} & \dfrac{\partial Q_k}{\partial V_{shu}}V_{shu} & \dfrac{\partial Q_k}{\partial V_m}V_j & \dfrac{\partial Q_k}{\partial \delta_{se}} & \dfrac{\partial Q_k}{\partial V_{se}}V_{se} & \dfrac{\partial Q_m}{\partial \delta_{shu}} \\[2ex] \dfrac{\partial Q_m}{\partial \delta_k} & \dfrac{\partial Q_m}{\partial \delta_m} & 0 & \dfrac{\partial Q_m}{\partial V_m}V_m & \dfrac{\partial Q_m}{\partial \delta_{se}} & \dfrac{\partial Q_m}{\partial V_{se}}V_{se} & 0 \\[2ex] \dfrac{\partial P_{mk}}{\partial \delta_k} & \dfrac{\partial P_{mk}}{\partial \delta_m} & 0 & \dfrac{\partial P_{mk}}{\partial V_m}V_m & \dfrac{\partial P_{mk}}{\partial \delta_{se}} & \dfrac{\partial P_{mk}}{\partial V_{se}}V_{se} & 0 \\[2ex] \dfrac{\partial Q_{mk}}{\partial \delta_k} & \dfrac{\partial Q_{mk}}{\partial \delta_m} & 0 & \dfrac{\partial Q_{mk}}{\partial V_m}V_m & \dfrac{\partial Q_{mk}}{\partial \delta_{se}} & \dfrac{\partial Q_{mk}}{\partial V_{se}}V_{se} & 0 \\[2ex] \dfrac{\partial P_{bb}}{\partial \delta_k} & \dfrac{\partial P_{bb}}{\partial \delta_m} & \dfrac{\partial P_{bb}}{\partial V_{shu}}V_{shu} & \dfrac{\partial P_{bb}}{\partial V_m}V_m & \dfrac{\partial P_{bb}}{\partial \delta_{se}} & \dfrac{\partial P_{bb}}{\partial V_{se}}V_{se} & \dfrac{\partial P_{bb}}{\partial \delta_{shu}} \end{bmatrix} \tag{12}$$

3. Loading Parameters and Continuation Power Flow

3.1 Loading Parameter

The most widely accepted assessment method for voltage collapse is the bifurcation theory. It is a suitable mathematical hypothesis capable of classifying stability issues. The theory can evaluate the system performance near failure or unstable points, providing quantifiable data on countermeasures to mitigate critical situations [14]. The bifurcation theory states that system formulas depend on several factors as well as model state parameters [15]:

$$\psi(\rho, \lambda) = 0 \tag{13}$$

where, ρ is a state variable of the power system; λ is the loading parameter.

Properties of stability or instability can be evaluated by gradually changing the settings. The loading parameter λ is introduced to assess if a system is in danger of voltage collapse. The load values are changed as follows:

$$P_{Li} = (1 + k_{ip}\lambda)P_{L0i} \tag{14}$$

$$Q_{Li} = (1 + k_{iq}\lambda)Q_{L0i} \tag{15}$$

where, P_{L0i} and Q_{L0i} are the active and reactive powers at fundamental operating point of the bus, respectively; k_{ip} and k_{iq} are the load distribution factors.

Voltages are typically depicted as functions of, or the measures of system loadability. In bifurcation diagrams, they are illustrated by P-V or nose curves. Eqns. (14) and (15) can be applied to the CPF analysis [14].

3.2 Continuation Power Flow

The nose slopes of electrical transmission lines can be determined using CPF techniques, which are also useful for estimating scenarios with high loading and "critical" requirements (for example, saddle-node and points of bifurcation caused by limits). The CPF method used in this study can distinguish between a P-V graph's stable and unstable areas. It is unaffected by numerical instabilities. Furthermore, it can provide information like the sensitivity of the current resolution to important parameters [14].

In static and dynamic voltage stability investigations, the CPF, which from a mathematical standpoint is a homotopy technique [14], can examine the stability of power system formulas, when a system variable is changed. It is commonly the loading parameter.

Typically, the CPF consists of two stages: the predictor stage, which is attained through the calculation of the tangent vector, and the calibration stage, which can be attained through either a local characterization or a

perpendicular crossing.

A typical CPF approach with predictor and corrector phases is shown in Figure 3 as an iterative process.

By means of a step that employs a tangent predictor, an estimation of the resolution point B for a given load route denoted by is carried out starting from a recognized initial position A. After that, using the corrector step, a power flow and an additional formula are used to establish the precise solution C.

This procedure is repeated until the desired bifurcation graph or P-V curve is obtained.
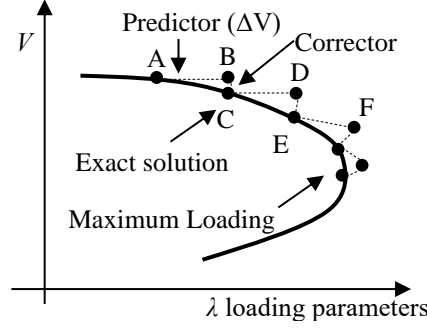

Figure 3. The CPF technique

4. Simulation Results

Our simulation targets the IEEE 14-, 30-, and 57-bus systems. Specifically, the 14-bus system has 20 lines and 5 generators, the 30-bus system has 41 lines and 6 generators, and the 57-bus system has 80 lines and 7 generators [16]. The UPFC location was taken from earlier investigations [17, 18].

The CPF was performed on the test systems with and without the UPFC to see the effect of such device on voltage stability (Figures 4-9).
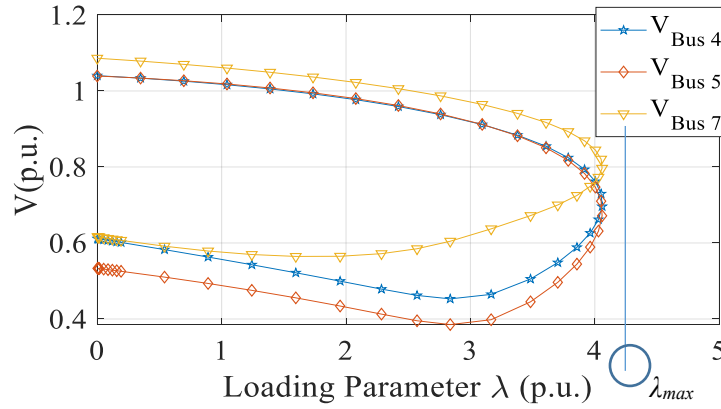

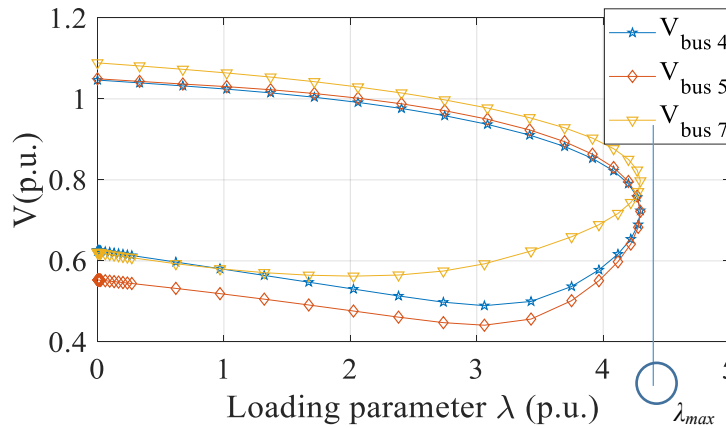**Figure 4.** P-V curve for the 14-bus test system without UPFC
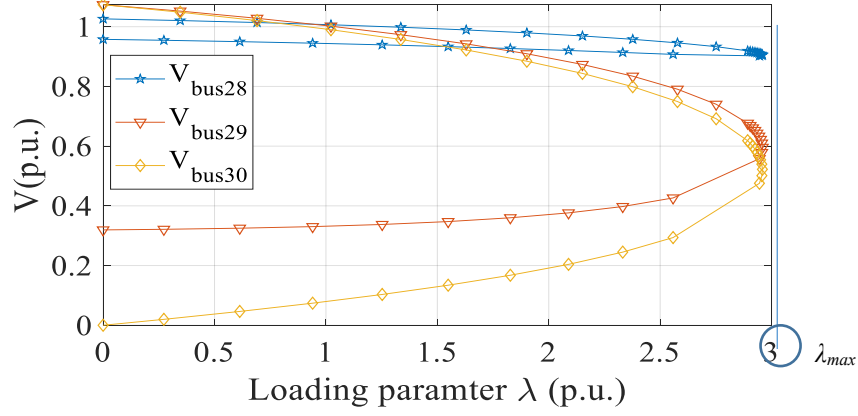

Figure 5. P-V curve for the 14-bus test system with UPFC

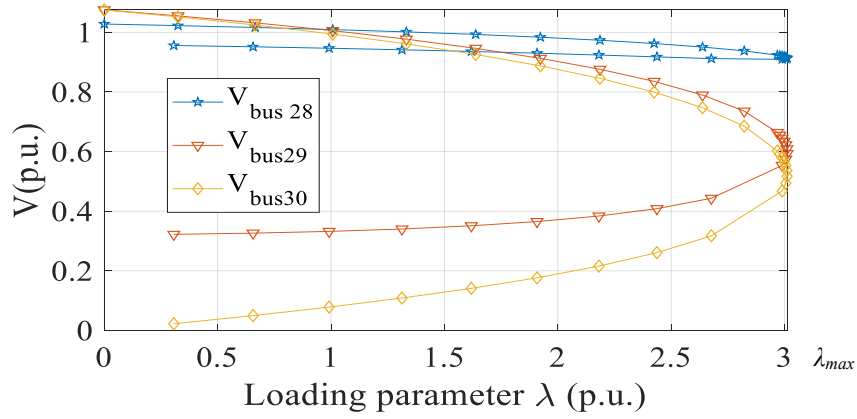**Figure 6.** P-V curve for the 30-bus test system with UPFC

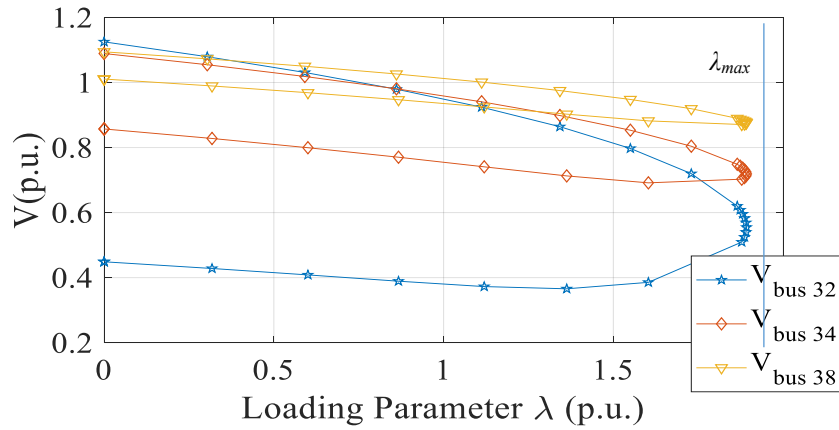**Figure 7.** P-V curve for the 30-bus test system without UPFC

Figure 8. P-V curve for the 57-bus test system without UPFC

From Figures 4-9, it can be seen clearly that the loading parameter λ is greater for the test systems with UPFC than those without UPFC. The reason is that the maximum loading point is pushed further by using the UPFC, which thus enhances the voltage stability. Table 1 lists the loading parameters values with and without UPFC for the test systems.

The maximum loading parameter before the system loses stability is shown in Table 1. The higher the value, the more voltage stability margin the system has. It is evident that the loading parameter value is higher in all test systems with the UPFC, and that as test system size is increased, the difference in values becomes less pronounced. The load is multiplied by the loading parameter each time, and the greater the load, the greater the system's capacity to deliver additional load without losing stability.

The amount of additional load that can be added to the 14-bus test system without it losing stability is increased by 16% utilizing the UPFC, the amount of power is improved by 15% for the 30-bus test system, and the amount is reduced by 7% for the 57-bus test system.
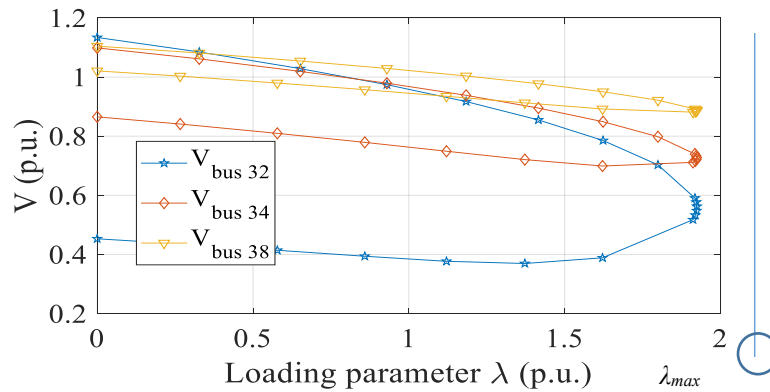

Figure 9. P-V curve for the 57-bus test system with UPFC

Table 1. Loading parameter values with and without UPFC

λ_{max}	Without UPFC	With UPFC
14 Bus	2.9588	3.0066
30 Bus	1.8921	1.9201
57 Bus	3.187	3.1895

5. Conclusion

This study carries out the CPF analysis to evaluate the impact of UPFC on the voltage stability of power systems. Firstly, the modeling technique is presented through the modified power flow equations and Jacobian matrix. To determine the point of voltage collapse, the model is implanted through the CPF analysis, which multiplies the loading parameter by the load active and reactive powers. Next, the efficiency of the UPFC in improving voltage stability is validated through a simulation on numerous IEEE test systems. The simulation shows that the UPFC pushes further the point of collapse, allowing the power system to supply more power and bear greater loads.

Data Availability

The data used to support the findings of this study are available from the corresponding author upon request.

Conflicts of Interest

The authors declare that they have no conflicts of interest.

References

[1] S. Parvathy, K. S. Thampatty, and T. P. Nambiar, "Analysis and modeling of UPFC: A comparison between power injection model and voltage source model," In 2017 IEEE Region 10 Symposium, Cochin, India, July 14-16, 2017, IEEE, pp. 1-5. https://doi.org/10.1109/TENCONSpring.2017.8070110.
[2] A. S. Geethu and K. C. Thampatty, "Design and implementation of series connected FACTS devices for Enhancing powersystem oscillation damping," *Int J. Adv Infor. Eng. Technol.*, vol. 3, no. 6, pp. 13-20, 2016.
[3] M. Chakravorty and S. Patra, "Voltage stability analysis using conventional methods," In 2016 International Conference on Signal Processing, Communication, Power and Embedded System, Paralakhemundi, India, October 3-5, 2016, IEEE, pp. 496-501. https://doi.org/10.1109/SCOPES.2016.7955879.
[4] S. Parvathy, K. C. Sindhu Thampatty, and T. N. Padmanabhan Nambiar, "Response of voltage source model of UPFC in an IEEE 5 bus system for power flow enhancement," In 2017 International Conference on Technological Advancements in Power and Energy, Kollam, India, December 21-23, 2017, IEEE, pp. 1-5. https://doi.org/10.1109/TAPENERGY.2017.8397279.
[5] B. Mewara, A. Bhargava, and K. Jain, "DPFC performance for improvement of power quality in power system undergoing unbalance faulty condition," In 2018 International Conference on Inventive Research in

Computing Applications Coimbatore, India, July 11-12, 2018, IEEE, pp. 704-708. https://doi.org/10.1109/ICIRCA.2018.8597242.

[6]   S. Slochanal, S. Latha, and K. Chithiravelu, "A novel approach of power flow analysis incorporating UPFC," In 2005 International Power Engineering Conference, Singapore, November 2, 2005, IEEE, pp. 701-704. https://doi.org/10.1109/IPEC.2005.206998.

[7]   R. M. Pereira, A. J. Pereira, C. M. Ferreira, and F. M. Barbosa, "FACTS performance in the dynamic voltage stability of an electric power system," In 2017 52nd International Universities Power Engineering Conference, Heraklion, Greece, August 28-31, 2017, IEEE, pp. 1-5. https://doi.org/10.1109/UPEC.2017.8231898.

[8]   Z. Fei, C. Guo, L. Jiang, L. Yang, and J. Zhang, "The multi-objective voltage stability coordinated control strategy of FACTS," In 2013 IEEE Power & Energy Society General Meeting, Vancouver, BC, July 21-25, 2013, IEEE, pp. 1-5. https://doi.org/10.1109/PESMG.2013.6672642.

[9]   F. Aydin and B. Gumus, "Determining optimal SVC location for voltage stability using multi-criteria decision making based solution: Analytic hierarchy process (AHP) approach," *IEEE Access*, vol. 9, Article ID: 143166, 2021. https://doi.org/10.1109/ACCESS.2021.3121196.

[10]   X. P. Zhang, C. Rehtanz, and B. Pal, Flexible AC Transmission Systems: Modelling and Control, Berlin Heidelberg: Springer-Verlag, 2012.

[11]   C. Fuerte-Esquivel and E. Acha, "Unified power flow controller: A critical comparison of Newton-Raphson UPFC algorithms in power flow studies," *IEE P-Gener. Transm. D.*, vol. 144, no. 15, pp. 437-444, 1997. https://doi.org/10.1049/ip-gtd:19971385.

[12]   E. Acha, C. R. Fuerte-Esquivel, H. Ambriz-Pérez, and C. Angeles-Camacho, FACTS Modelling and Simulation in Power Networks, England: Wiley, 2004.

[13]   S. E. Mubeen, R. K. Nema, and G. Agnihotri, "Comparison of power flow control: TCSC versus UPFC," In 2008 Joint International Conference on Power System Technology and IEEE Power India Conference, New Delhi, India, October 12-15, 2008, IEEE, pp. 1-5. https://doi.org/10.1109/ICPST.2008.4745238.

[14]   O. L. Bekri, M. K. Fellah, M. F. Benkhoris, and A. Miloudi, "Voltage stability enhancement by optimal SVC and TCSC location via CP flow analysis," *Int Rev. Electr. Eng-I.*, vol. 5, no. 15, pp. 2263-2269, 2010.

[15]   D. Devaraj and R. Jeevajyothi, "Impact of wind turbine systems on power system voltage stability," In 2011 International Conference on Computer, Communication and Electrical Technology, Tamilnadu, India, March 18-19, 2011, IEEE, pp. 411-416. https://doi.org/10.1109/ICCCET.2011.5762510.

[16]   "Power systems test case archive," Washington University, 2022, https://labs.ece.uw.edu/pstca/.

[17]   D. K. Y. Islam, H. Samir, and D. M. Abdeldjalil, "Study of UPFC optimal location considering loss reduction and improvement of voltage stability and power flow," *Leonardo J. Sci.*, vol. 13, no. 12, pp. 85-100, 2014.

[18]   Y. I. Djilani Kobibi, "Incorporation de l'UPFC dans le calcul de la répartition des puissances dans un réseau électrique," Ph.D. Dissertation, Djillali Liabes University, Algeria, 2016.